The final publication is available at

https://doi.org/10.1111/1750-3841.15094

Additional Information

Polylactic acid based materials encapsulating carvacrol obtained by solvent casting and electrospinning

Alina Tampau [a], Chelo González-Martínez [b], Amparo Chiralt [c]

[a, b, c] Universidad Politécnica de Valencia, Valencia, Spain

Contact information for Corresponding Author

Alina Tampau

Mailing address: Instituto Universitario de Ingeniería de Alimentos para el Desarrollo, Ciudad Politécnica de la Innovación, building 8E Access F, L0-03, Universitat Politécnica de Valencia, Camino de Vera, s/n, 46022 Valencia, Spain.

E-mail address: altam@upv.es

Word count of text: 5412 words

Short version of title: Carvacrol-loaded PLA matrices (…)

Choice of journal/topic where article should appear:

Journal of Food Science: Food Engineering, Materials Science, and Nanotechnology

ABSTRACT

Polylactic acid (PLA) dissolved (15 wt. %) in ethyl acetate (EtAc) : dimethyl sulfoxide (DMSO) binary systems (0:1; 1:3 and 2:3 v/v) was used as carrier to obtain Carvacrol (CA) loaded (20 wt. % with respect to PLA) matrices by electrospinning, in comparison with solvent casting. Field Emission Scanning Electron Microscopy (FESEM) observations showed that CA-loaded electrospun fibers were thinner than the CA-free ones and their encapsulating efficiency (EE) increased when EtAc was present in the solvent. The cast films had higher EE (up to 89 %) than the electrospun mats (max. 68 %). Thermogravimetric analysis and differential scanning calorimetry revealed that CA-free matrices retain more solvent than the samples with CA, this effect being more noticeable in fibers rather than in cast films. The thermal analysis revealed stronger retention forces of CA in the fibers than in the cast material and the carvacrol plasticizing effect in the PLA matrices, in accordance with its retained amount.

Practical Application:

The carvacrol-loaded polylactic acid materials obtained in this study are intended to serve as possible active layer in obtaining active (antimicrobial and/or antioxidant) multilayer materials for the packaging of foodstuffs, when applied onto a supporting polymer layer. Active properties of the material, as well as the potential carvacrol sensory impact, in packaged products should be assessed in further studies.

1 Introduction

Traditionally, the functions of food packaging were protection, communication, containment and transport safety. However, innovation in food packaging has been directed towards the development of new technologies that provide additional benefit, such as the so-called active and intelligent packaging (Martínez-Tenorio & López, 2011). The active packages (Regulation (EC) No. 450/2009 (EU, 2009)) can be obtained either by introducing the active element into the package together with the product or by introducing the active agent into the packaging material itself. This second option would be the most attractive from the consumer's point of view, as nothing strange would be found inside the packaging that would attract attention and cast doubt on the quality of the food (Catalá & Gavara, 2001).

In regards to food preservatives, due to growing consumer concern about synthetic ingredients, the use of natural active compounds extracted from plants represents an attractive alternative in active packaging materials for foods. Of these components, carvacrol (CA), a phenolic monoterpenoid abundant in oregano and thyme essential oils (De Vincenzi, Stammati, De Vincenzi, & Silano, 2004), is one of the most active in terms of antioxidant and antimicrobial activity and approved by the EFSA (2012) as a food flavoring agent. Despite its proven efficacy, carvacrol's use in active packaging materials is limited due to different drawbacks, such as its high volatility (Turek & Stintzing, 2013), low water solubility (1250 mg/L, Yalkowsky, He, & Jain, 2010) and high sensory impact (Hsieh, Mau, & Huang, 2001). Carvacrol encapsulation in a polymeric matrix could enhance the protection of the compound, mitigate its sensory impact and control its release from the material to develop its active functions (Majeed et al., 2015). Ramos, Jiménez, and Garrigós (2016) reviewed different studies and reported on the incorporation of carvacrol into synthetic polymers and biopolymers to obtain innovative materials for active food packaging.

86 One potential strategy to develop active packaging consists of obtaining multilayer materials in

87 which polymers with complementary properties are assembled to meet the food packaging

88 requirements, in terms of barrier capacity against water vapor or gases, while the active

89 compound could be incorporated in one of the layers. To this end, one possibility is the extension

90 of a polymeric layer containing the active compound over a supporting packaging material, and

91 the subsequent evaporation of the solvent (casting method) (Rhim, Mohanty, & Singh, 2005).

92 With this technique, Busolo, Fernandez, Ocio, and Lagaron (2010) obtained high water barrier

93 PLA chloroform-cast films encapsulating a silver-based nanoclay with strong antimicrobial

94 activity. However, one of the shortcomings of casting is the effective extension of the active-

95 polymer solution on the polymeric support layer. This process requires a high wettability of the

96 polymeric support with the cast solution that is greatly affected by the chemical affinity of the

97 solution and supporting layer, and their surface properties. Also, casting involves the evaporation

98 of large amounts of solvent that constitute a limitation at the industrial level. Electrospinning

99 (ES) is an alternative technique for depositing an active polymer layer on a polymeric sheet in

100 order to obtain multilayer materials. The ES technique uses an electric field to produce the

101 stretching of the polymeric solution. This allows the solvent in the sample stream to evaporate

102 progressively due to the large contact area between the stream surface and air. Then the electro-

103 drawn material reaches the collector in a dry state, producing nano or microfibers (Bhardwaj &

104 Kundu, 2010). With this technique, polymer meshes with a high surface area / volume ratio, and

105 very small pores are obtained (Liang, Hsiao, & Chu, 2007).

106 To reduce the environmental impact of synthetic plastics (García, 2004), the use of biodegradable

107 polymers in the development of active food packaging is necessary. Of the available

108 biodegradable materials, polylactic acid (PLA) is an interesting option since it is a biodegradable

109 polyester obtained from the microbial fermentation of renewable sources with high

110 carbohydrate content (Serna, Rodríguez, & Albán, 2003), and it is approved by the Food and Drug

111   Administration (FDA, US) as food contact material. Previous studies reported the use of PLA in

112   electrospun matrices, using solvents unfit for food contact. Alharbi, Luqman, Fouad, Khalil, and

113   Alharthi (2018) obtained PLA-core/PVA-shell coaxially spun nanofibers, using chloroform:

114   dimethylformamide (8:2) as solvent for the polylactide. The core/shell composites exhibited

115   higher tensile strength and ductility than the pristine PLA fibers. Likewise, Li, Frey, and Baeumner

116   (2006) successfully obtained PLA electrospun mats incorporating biotin -- intended as

117   membranes for biosensors -- using chloroform: acetone (3:1) as solvent. A good distribution of

118   the biotin along the length of the individual fibers was achieved, making it accessible for binding

119   with the streptavidin used as detector of *E. coli.* Scafarro, Maio, and Lopresti (2019) obtained cast

120   and electrospun materials with PLA, CA and graphene nanoplatelets (GNP), using chloroform-

121   acetone mixtures. They reported that the incorporation of GNP strengthened and stiffened the

122   cast films, whereas it had an opposite effect in the electrospun fibrous mats, decreasing their

123   stiffness. Likewise, the CA amount and release kinetics could be modulated by the GNP,

124   prolonging the active's release time, making this kind of materials useful for applications in

125   wound dressing or scaffolds for neuronal tissue engineering.

126   The aim of this study was to assess the capability of electrospun PLA matrices to encapsulate

127   carvacrol in comparison with cast obtained films, by using different solvent systems approved for

128   food contact. The obtained materials were characterized as to their encapsulation efficiency,

129   microstructure and thermal behavior.

130   **2 Materials and Methods**

131   **2.1. Materials**

132   Amorphous polylactic acid (PLA) 4060D, with a density of 1.24 g/cm^3, was obtained from

133   NatureWorks (Minnesota, USA) while carvacrol (CA) was supplied by Sigma-Aldrich (Steinheim,

134   Germany). As for the solvents used, dimethyl sulfoxide (DMSO), glacial acetic acid (GAA) and

135 absolute ethanol were purchased from Panreac Química S.L.U. (Castellar del Vallès, Barcelona,

136 Spain); butyl acetate (ButAc) was purchased from Sigma-Aldrich (Steinheim, Germany) and ethyl

137 acetate (EtAc) from Indukern (El Prat de Llobregat, Barcelona, Spain).

138 **2.2. Obtaining the CA encapsulating matrices**

139 15 wt. % PLA solutions (with or without 20 wt. % CA with respect to the polymer) were prepared

140 by placing the PLA pellets in the selected solvent systems in hermetically sealed recipients and

141 maintaining under magnetic stirring at room temperature (25 ± 1 °C) for 24 h to ensure complete

142 dissolution. The ratio carvacrol-polymer has been chosen, on the basis of previous studies

143 (Tampau, González-Martínez, & Chiralt, 2018) to ensure enough load of carvacrol in the matrix

144 to exert its antimicrobial action when applied in the packaging films. Initially, EtAc was used in

145 order to meet the requirements for food contact use. Nevertheless, to solve the problems

146 associated with its fast evaporation at the tip of the spinneret, other solvents (DMSO, GAA and

147 ButAc) with higher boiling points were considered as co-solvents on the basis of their miscibility

148 with the EtAc and good solvent properties with respect to PLA (Scharlab, 2018). The properties

149 of the chosen solvents, relevant for the electrospinning process, as well as the binary

150 combinations tested, are given in **Table 1**.

151 The electrospinning of the polymer solutions was carried out under ambient conditions (25 ± 1

152 °C, 45 % relative humidity (RH)) in Fluidnatek equipment (Bioinicia S.A., Valencia, Spain) with

153 mono and coaxial mode. In the co-axial mode, only the solvent of the respective polymeric

154 solution passes through the exterior needle. The process parameters (flow rate, injector-collector

155 distance and voltage) were empirically adjusted to ensure a stable "Taylor cone" formation at the

156 tip of the spinneret. They were fitted on the basis of the previous screening with different solvent

157 systems. For the selected solvents, the PLA solutions were electrodeposited for 1 hour at a flow

158 rate of 1.0 mL/h. The material was deposited on sheets of aluminum foil (previously weighed)

159 placed on the collector, 20 cm from the spinneret tip. The voltage (13.5-15 kV) was adjusted

160 depending on the solution. The obtained material was preserved until its characterization in

161 vacuum desiccators with silica gel to favor further drying and avoid moisture absorption.

162 The same selected solutions were used to obtain cast materials. These were poured onto Teflon

163 plates of 15 cm in diameter to obtain a surface solid density of $5.6 \cdot 10^{-3}$ g polymer / cm^2 and

164 placed in a fume hood for solvent evaporation and film formation. The films were peeled from

165 the plate and stored in a vacuum desiccator, with silica gel, until their characterization.

166 **2.3. Characterization of the obtained materials**

167 **2.3.1. Microstructure**

168 The obtained ES and cast matrices were observed with a Field Emission Scanning Electron

169 Microscopy equipment (FESEM Ultra 55, Zeiss, Oxford, UK). The samples were mounted with

170 carbon tape on supports and, after being vacuum coated with platinum, were observed using an

171 acceleration voltage of 1 kV. Image analysis, using the ImageJ software (National Institutes of

172 Health, USA), was carried out to measure the size of fibers in the obtained electrospun structures.

173 At least 25 measurements of the fibers were considered per formulation.

174 **2.3.2. CA encapsulating efficiency**

175 The CA retention of the matrices was assessed by means of the ethanol extraction of carvacrol

176 and spectrophotometric determination at 275 nm, using a UV/Vis spectrophotometer (Evolution

177 201 UV-Vis, Thermo Fisher Scientific Inc.), as previously described by Tampau, González-Martínez

178 and Chiralt (2017). Briefly, electrospun samples (deposited on aluminum foils) or cast film

179 fragments (about 3-5 mg) were introduced into absolute ethanol (15 mL) in amber bottles that

180 were hermetically sealed and kept under stirring for 24 h at room temperature (25 ± 1 ^{o}C). The

181 absorbance of the extracts was measured using the respective extract of the CA-free matrix as

182 background. Carvacrol concentration was determined as µg CA/mL, using a calibration curve

183 obtained for CA solutions with 10-85 µg/mL (Concentration= $67.325 \cdot$ Absorbance, R^2=0.998). The

184   encapsulating efficiency (EE) was expressed as the percentage (%) of total ethanol-extracted CA

185   with respect to the theoretical CA content. Each formulation was analyzed in triplicate.

186   **2.3.3. Thermal analysis**

187   Previously P_2O_5-conditioned samples were submitted to thermal analyses in order to assess the

188   effect of the carvacrol and processing method on phase transitions and thermal stability of the

189   matrices.

190   Thermogravimetric analysis (TGA), evaluating the thermal degradation of the material, was

191   performed using a thermogravimetric analyzer (TGA/SDTA 851e, Mettler Toledo,

192   Schwarzenbach, Switzerland). Samples placed into an alumina crucible were heated at a rate of

193   10 K/min from 25 °C to 700 °C under inert nitrogen atmosphere (flow 20 mL/min). DTA and DGTA

194   curves were analyzed, and the onset (T_o) and peak (T_p) temperatures for the different mass loss

195   steps were determined, as well as the relative mass loss in the first step.

196   Differential scanning calorimetry (DSC) analyses were carried out using a DSC (1 StarE System,

197   Mettler-Toledo, Inc., Switzerland). The samples (5-10 mg) were placed into aluminum pans (Seiko

198   Instruments, P/N SSC000C008) and sealed. The samples, initially maintained at -25 °C for 5 min,

199   were heated to 225 °C, then cooled to -25 °C, kept at -25 °C for 5 min and heated again to 275

200   °C. The thermal scanning was performed at 10 K/min. As reference, an empty aluminum pan was

201   used. The thermograms were processed using the software of the equipment (Mettler-Toledo,

202   Inc., Switzerland) to determine the glass transition (T_g) temperatures. The thermal analyses (TGA

203   and DSC) of the samples were carried out in triplicate.

204   **2.4. Statistical analysis**

205   All the data were processed using the software Statgraphics Centurion XVI (Statpoint

206   Technologies Inc., VA, USA) and applying analysis of simple variance (ANOVA). Fisher's least

207   significant difference (LSD) (with a 95.0 % confidence level) was used in order to identify

208   significantly different samples. DSC data were also analyzed using a multifactor analysis of

209 variance with 95 % significance level, considering the presence of CA in the matrix and the

210 processing method (C or ES) as factors.

3 Results and Discussion

3.1. Solvent system screening

213 Electrospinning of the 15 wt. % PLA dissolved in pure EtAc revealed the obstruction of the

214 spinneret after about 10 min processing due to the solidification of the polymer. This was

215 attributed to the low boiling point (**Table 1**) of the solvent which promoted an overly fast

216 evaporation rate. Combination of EtAc with other solvents with higher boiling points (**Table 1**)

217 and the coaxial mode of the process were tested to mitigate this problem, fitting the process

218 conditions to obtain a stable Taylor cone. **Table 1** shows the fitted conditions, including or not

219 co-axial flow, established for each binary solvent system, as well as the processing time during

220 which no problems occurred with the jet flow.

221 It was observed that the use of DMSO in the solvent mixture allowed for a much longer duration

222 of the process than with the rest of the solvents, without solidification at the tip of the injector

223 (**Table 1**). However, the electrospun material was not completely free of solvent once the process

224 was finished; the mats collected from the ES equipment produced a wet, translucent appearance.

225 Blends of EtAc and GAA (1:1, v/v) were also tested on the basis of their higher boiling point, and

226 good solvent properties of GAA (parameter of Flory-Huggins<0.5; Casasola, Thomas, &

227 Georgiadou, 2016). However, this blend did not extend the useful process time enough, with or

228 without coaxial flow (**Table 1**). The solutions using EtAc:GAA 2:1 and 4:1 and EtAc:ButAc 1:1

229 exhibited an opalescent appearance, which indicated a partial dissolution of the polymer, and

230 were therefore discarded for their subsequent use.

231 The microstructural characteristics of the obtained fibers under the different operating

232 conditions reflected in **Table 1** are shown in **Figure 1**. In most cases, fibers with elongated

233 droplets were obtained, depending on the solvent and process conditions. The samples obtained

234 with co-axial solvent flow presented less fiber formation with a higher proportion of beads, in

235 accordance with the drop in the polymer concentration at the spinneret needle, due to a local

236 dilution induced by the outer flow of solvent. Yu, Li, Ge, Ye, & Wang (2013) also observed this

237 effect for co-axial electrospinning of ethyl cellulose from an ethanol solution, using a sheath of

238 solvent through the outer needle. When the solvent sheath flowrate was above a certain ratio

239 with respect to the solution flowrate, the electrospun fibers presented beads-on-string

240 morphology.

241 Therefore, based on the observed morphology of the material and the processing time without

242 partial solidification at the injector tip, three EtAc:DMSO mixtures (0:1, 1:3 and 2:3) were chosen

243 for further studies encapsulating carvacrol, by processing in monoaxial application mode. The

244 distance between the injector and the collector was set at 20 cm and the voltage adjusted to

245 achieve a stable application (between 14 and 18 kV, depending on the solvent).

246 **3.2. Microstructure of the ES matrices**

247 With the selected binary solvent systems, matrices of PLA with and without encapsulated CA

248 were obtained, in mono-axial mode, whose micrographs obtained by FESEM are shown in **Figure**

249 **2**. Fiber mats with few beads were obtained in all cases. The relatively flat structure of the

250 obtained fibers revealed the lack of a complete solvent evaporation. The residual solvent

251 plasticized the material and provoked its flattening on the collector surface.

252 The incorporation of carvacrol modified the structure of the electrospun material, mainly in the

253 sample obtained with pure DMSO, where it presents a compact appearance likely attributable to

254 fibers not being completely dry when deposited in the mesh on the collector. Except when

255 solvent was pure DMSO, the presence of the CA promoted the formation of thinner fibers than

256 those obtained for the respective CA-free controls **(Figure 2)**. This could be related to the

257 modification of the interactions between the chains of the polymer allowing a greater stretching

258   of the fiber in the electric field. It can be observed in the micrographs that by increasing the

259   proportion of EtAc in the solvent mixture, fibers with larger diameters were obtained, an effect

260   verified by the image analysis results shown in **Figure 2**. This was consistent with the observations

261   reported by other authors (Wannatong, Sirivat, & Supaphol, 2004; Casasola, Thomas, Trybala, &

262   Georgiadou, 2014) who attributed this effect to the lower boiling point of the solvent. The higher

263   the boiling point during electro-stretching, the longer the fiber remains wet, and the more it

264   stretches in the electric field.

265   **3.3. Carvacrol encapsulating efficiency**

266   **Table 2** shows the encapsulation efficiency (EE) for the different materials obtained by ES and

267   casting. The EE values reflected a greater CA retention capacity in the matrix when the casting

268   method was used. Likewise, the electrospun fibers obtained from the bisolvent mixtures

269   presented higher encapsulating efficiency than those obtained with pure DMSO. This could be

270   attributed to faster solvent evaporation in the mixtures with EtAc that enhanced the solidification

271   of the polymer fiber, entrapping the active compound and preventing its evaporation. Therefore,

272   the lower boiling point of the solvent caused the formation of thicker fibers, as previously

273   discussed, with higher carvacrol content. In cast films, lower differences in the EE associated with

274   the solvent boiling point were observed, probably due to the fact that the evaporation of the

275   solvent occurs at the film surface, with much lower specific area.

276   **3.4. Thermal analysis**

277   **Figure 3** and **Table 3** present the results of the thermogravimetric analysis that showed two

278   weight loss stages, as observed in the TGA curves. The first degradation step of less intensity, up

279   to temperatures of about 150 °C (in CA-free samples) or 250 °C (in samples with CA), must be

280   attributed to the thermo-release of solvent residues or both solvent and encapsulated CA,

281   respectively. In fact, the peak temperature of this step was higher in samples containing

282   carvacrol, coherently with the higher volatilization temperature of this compound. The second

step, at higher temperatures, much more intense, corresponded to the thermo-degradation of the polymer. During the first stage, variable mass losses were detected depending on the sample. Losses of up to 40 % (**Table 3**) occurred in fibers without CA and indicate the retention of a large amount of solvent in the matrix that is released during heating. This retention increased with the content of EtAc in the solvent mixture. This suggests the appearance of specific interactions of the solvent with the polymer, which limit its evaporation during electrospinning. This solvent retention effect was also observed in casting films for the solvent EtAc:DMSO with ratio of 1:3 and was very slight for the 2:3 mixture and pure DMSO. In the samples carrying carvacrol, the first stage of weight loss extends to higher temperatures, given the higher boiling point of carvacrol compared to DMSO, and was more intense for casting films than for fibers. This could be related with the highest content of carvacrol retained in the film determined by spectrophotometry (**Table 2**). It is remarkable that the presence of CA seems to minimize the solvent retention since the mass loss occurs mainly in the temperature range corresponding to the release of carvacrol. In fact, assuming that the mass loss of the first temperature interval, corresponds to the thermo-release of carvacrol before the polymer degradation, it can be deduced that only a fraction of the encapsulated compound was delivered from the fibers, since the weight loss was lower than the corresponding total carvacrol content determined by spectrophotometry. This suggests that a part of the carvacrol (about 60 % of the total) was strongly bonded to the polymer and was not thermo-released before the polymer degradation. However, in cast samples, the mass loss that occurred during the first step was, in general, slightly higher than the carvacrol content in the samples, which indicates that a part of the thermo-released mass must also correspond to adsorbed solvent. This mainly occurred when solvent contained EtAc, which concurs with what was observed for carvacrol-free materials that retained significant amounts of solvent when there was more ratio of EtAc in the mixture.

307 The degradation step of the polymer occurred in a temperature range that was affected by the

308 type of processing and the presence or absence of carvacrol. In CA-loaded cast material, the

309 temperature of the degradation peak increased when the EtAc ratio in the solvent rose and

310 reached values higher than those of the polymer pellets, whereas the opposite effect was

311 observed with cast samples without carvacrol. In contrast, no significant effect of solvent was

312 observed in the temperature peak of electrospun material with or without carvacrol.

313 Nevertheless, carvacrol-loaded mats exhibited lower peak temperature than carvacrol free ones.

314 These results suggested that in the obtained matrices the interactions of the residual solvent or

315 carvacrol with the polymer chains affected the degree of packing of the chains in the matrix,

316 giving rise to structures with different thermal resistance. The greater the polymer matrix's

317 degree of compactness, the higher the expected degradation temperature of the matrix is. On

318 the other hand, the presence of carvacrol affected the interactions of the chains with the solvent,

319 leading to lower solvent adsorption in the polymer matrix, especially in the electrospun material.

320 These results indicate that the polymer chains in amorphous PLA interact specifically with the

321 solvent (EtAc and DMSO) molecules and carvacrol, which affects the retention of these

322 compounds in the matrix and its compactness. This, in turn, determines the thermal degradation

323 temperature of the polymer. The effects of the solvent were more relevant in the absence of

324 carvacrol, notably in fibers. This could be attributed to the blocking of the active points of the

325 chains through preferential interactions with carvacrol, thus limiting their ability to interact with

326 the solvent molecules and limiting the solvent retention in the material.

327 The first heating scans in the DSC thermograms exhibited endotherms associated with the

328 evaporation of the solvent retained in different proportions, as also deduced from the TGA

329 analyses. **Figure 4** shows an example of the obtained thermograms in the first heating scan for

330 the samples prepared by ES and casting, with and without carvacrol, using EtAc:DMSO (2:3)

331 where the solvent evaporation endotherms can be observed at different temperatures,

332 depending on the overpressure reached in the sample pan. The comparison of the vaporization

333 enthalpy with the enthalpy of the DMSO allowed to determine variable amounts of solvent,

334 depending on the analyzed sample. These enthalpies were greater in the samples without

335 carvacrol, revealing that the presence of the active substance contributes to a better evaporation

336 of the solvent from the fibers and the films, as previously deduced from the TGA analyses. It

337 reveals that the active points of the polymer for the solvent adsorption (interacting groups) are

338 shielded by the preferential interaction with carvacrol. In thermograms, the glass transition of

339 the polymer could be observed with the typical relaxation endotherm whose enthalpy values

340 ranged between 0.6 and 5.8 J/g, associated with aging of the matrix. As expected, this relaxation

341 no longer appears in the cooling sweep or in the second heating scan.

342 **Table 4** shows the T_g values of the different samples obtained in the heating (first and second)

343 and cooling scans. In general, the values for a determined sample in the cooling and the second

344 heating steps were higher than those of the first heating sweep. This reflects the plasticizing

345 effect of the adsorbed solvent in the initial sample. This solvent is released, at least partially,

346 during the first heating (as the endotherms shown in Figure 4 reveal). Then, the cooling or second

347 heating step could be considered to obtain the T_g of the samples when these were free of solvent

348 (after the first heating step). The variability observed in the values can be attributed to the

349 different proportions of solvent remaining in the samples during the different thermal steps, or

350 even to partial losses of carvacrol during the first heating. However, assuming the major release

351 of the solvent in the first heating scan, the T_g of the second heating scan was taken to estimate

352 the effect of CA on the T_g values. The average T_g values for all the ES samples containing carvacrol

353 was 37 ± 5 °C while for the cast samples with carvacrol, this value was 26 ± 8 °C. In contrast, for

354 all samples without CA the mean T_g was 44 ± 6 °C, which was in the range of the T_g obtained for

355 the non-processed polymer pellets (52 ± 2 °C). These values indicate that carvacrol had a

356 plasticizing effect on PLA, which will be affected by its load in the ES or cast matrices. The ES

samples with carvacrol exhibited higher T_g values than the carvacrol loaded cast samples, which is coherent with the lower amount of CA retained in the mats and so, the lower plasticizing effect of the retained compound.

4 Conclusion

The carvacrol encapsulation efficiency in PLA matrices was higher for solvent casting (76-89 %) than for electrospinning (52-68 %) and was affected by the ratio EtAc:DMSO in the solvent mixture. Nevertheless, fibers reached a carvacrol-load of 10-13 g per 100 polymer (against 15-18 in cast samples), from which only about 40 % was thermo-released before the polymer degradation, which indicates its strong retention in the fibers. In contrast, carvacrol was practically thermo-released in total in cast samples, which indicates lower retention forces in the matrix. As far as the solvent, the incorporation of the EtAc to DMSO significantly increased the encapsulating efficiency in the fibers (from 50 to almost 70 %), although in the cast samples a higher efficiency was only observed for the smallest ratio of EtAc. The electrospun material of PLA with or without carvacrol, using EtAc:DMSO mixtures as solvents, exhibited a fiber structure with few beads. Fiber diameter decreased when it contained carvacrol and increased when the proportion of EtAc in the solvent mixture rose. Based on the current study, electrospinning of solutions of PLA and carvacrol (20 wt. % with respect to the polymer) in mixtures of EtAc:DMSO (both valid for food contact) could be used effectively in obtaining active multilayer materials for the packaging of foodstuffs when applied onto a supporting polymer layer. Further studies would be necessary for assessing their antibacterial and antioxidant effects in different food substrates.

384

Author Contributions

386 A.Tampau: methodology, data collection and manuscript-original draft preparation.

387 C. González-Martínez and A. Chiralt: result interpretation, manuscript-review and editing.

388

Conflicts of Interest

390 There are no known conflicts of interest to declare.

391

References

393 Alharbi, H. F., Luqman, M., Fouad, H., Khalil, K. A., & Alharthi, N. H. (2018). Viscoelastic behavior

394 of core-shell structured nanofibers of PLA and PVA produced by coaxial electrospinning. Polymer

395 Testing, 67, 136–143. https://doi.org/10.1016/j.polymertesting.2018.02.026

396 Bhardwaj, N., & Kundu, S. C. (2010). Electrospinning: A fascinating fiber fabrication technique.

397 Biotechnology Advances, 28(3), 325–347. https://doi.org/10.1016/j.biotechadv.2010.01.004

398 Busolo, M. A., Fernandez, P., Ocio, M. J., & Lagaron, J. M. (2010). Novel silver-based nanoclay as

399 an antimicrobial in polylactic acid food packaging coatings. Food Additives & Contaminants: Part

400 A, 27(11), 1617–1626. https://doi.org/10.1080/19440049.2010.506601

401 Casasola, R., Thomas, N. L., Trybala, A., & Georgiadou, S. (2014). Electrospun poly lactic acid (PLA)

402 fibers: Effect of different solvent systems on fiber morphology and diameter. Polymer, 55(18),

403 4728–4737. https://doi.org/10.1016/j.polymer.2014.06.032

404 Casasola, R., Thomas, N. L., & Georgiadou, S. (2016). Electrospinning of poly (lactic acid):

405 Theoretical approach for the solvent selection to produce defect-free nanofibers. Journal of

406 Polymer Science, Part B: Polymer Physics, 54(15), 1483–1498.

407 https://doi.org/10.1002/polb.24042

408 Catalá, R., & Gavara, R. (2001). Nuevos envases. De la protección pasiva a la defensa activa de los

409 alimentos envasados. Arbor, 168(661), 109–127. https://doi.org/10.3989/arbor.2001.i661.825

410 De Vincenzi, M., Stammati, A., De Vincenzi, A., & Silano, M. (2004). Constituents of aromatic

411 plants: Carvacrol. Fitoterapia, 75(7–8), 801–804. https://doi.org/10.1016/j.fitote.2004.05.002

412 EC450. (2009). EC450, Regulation on active and intelligent materials and articles intended to

413 come into contact with food. Off J EU, 450(29 May 2009), L 135/3-135/11.

414 EFSA. (2012). Scientific Opinion on the Safety and efficacy of phenol derivates containing ring-

415 alkyl, ring-alkoxy and side- chains with an oxygenated functional group (chemical group 25) when

416 used as flavourings for all species. EFSA J., 10(2), 2573. https://doi.org/10.2903/j.efsa.2012.2573.

417 García, E. (2004). La civilización industrial y los límites del planeta. Medio Ambiente y Sociedad.,

418 59–99.

419 Hsieh, P. C., Mau, J. L., & Huang, S. H. (2001). Antimicrobial effect of various combinations of

420 plant extracts. Food Microbiology, 18(1), 35–43. https://doi.org/10.1006/fmic.2000.0376

421   Li, D., Frey, M. W., & Baeumner, A. J. (2006). Electrospun polylactic acid nanofiber membranes as

422   substrates for biosensor assemblies. Journal of Membrane Science, 279(1–2), 354–363.

423   https://doi.org/10.1016/j.memsci.2005.12.036

424   Liang, D., Hsiao, B. S., & Chu, B. (2007). Functional electrospun nanofibrous scaffolds for

425   biomedical applications. Advanced Drug Delivery Reviews, 59(14), 1392–1412.

426   https://doi.org/10.1016/j.addr.2007.04.021

427   Majeed, H., Bian, Y., Ali, B., Jamil, A., Majeed, U., Khan, Q. F., Fang, Z. (2015). Essential oil

428   encapsulations: uses, procedures, and trends. RSC Advances, 5(72), 58449–58463.

429   https://doi.org/10.1039/C5RA06556A

430   Martínez-Tenorio, Y., & López-Malo, A. (2011). Envases activos con agentes antimicrobianos y su

431   aplicación en los alimentos. Temas Selectos de Ingeniería De Alimentos, Vol. 2, pp. 1–12.

432   Retrieved from https://www.udlap.mx/WP/tsia/files/No5-Vol-2/TSIA-5(2)-Martinez-Tenorio-et-

433   al-2011.pdf

434   Ramos, M., Jiménez, A., & Garrigós, M. C. (2016). Chapter 26 - Carvacrol-Based Films: Usage and

435   Potential in Antimicrobial Packaging. In J. B. T.-A. F. P. Barros-Velázquez (Ed.), Antimicrobial Food

436   Packaging (pp. 329–338). https://doi.org/https://doi.org/10.1016/B978-0-12-800723-5.00026-7

437   Rhim, J. W., Mohanty, A. K., Singh, S. P., & Ng, P. K. W. (2006). Effect of the processing methods

438   on the performance of polylactide films: Thermocompression versus solvent casting. Journal of

439   Applied Polymer Science, 101(6), 3736–3742. https://doi.org/10.1002/app.23403

440   Scaffaro, R., Maio, A., & Lopresti, F. (2019). Effect of graphene and fabrication technique on the

441   release kinetics of carvacrol from polylactic acid. Composites Science and Technology,

442   169(October 2018), 60–69. https://doi.org/10.1016/j.compscitech.2018.11.003

443 Scharlab (2018, September 17). Retrieved from *http://scharlab.com/tabla-reactivos-*
444 *mezclabilidad.php*

445 Serna, L., Rodríguez, A., & Albán, F. (2003). Ácido Poliláctico (PLA): Propiedades y Aplicaciones.
446 Ingeniería y Competitividad, 5(1), 16–26.

447 Smallwood, I. M. (1996). Handbook of organic solvent properties. London: Arnold Hodder
448 Headline Group; New York: Halsted Press John Wiley & Sons.

449 Tampau, A., González-Martínez, C., & Chiralt, A. (2017). Carvacrol encapsulation in starch or PCL
450 based matrices by electrospinning. Journal of Food Engineering, 214, 245–256.
451 https://doi.org/10.1016/j.jfoodeng.2017.07.005

452 Tampau, A., González-Martínez, C., & Chiralt, A. (2018). Release kinetics and antimicrobial
453 properties of carvacrol encapsulated in electrospun poly-(ε-caprolactone) nanofibres.
454 Application in starch multilayer films. Food Hydrocolloids, 79, 158–169.
455 https://doi.org/10.1016/j.foodhyd.2017.12.021

456 Turek, C., & Stintzing, F. C. (n.d.). Stability of Essential Oils: A Review.
457 https://doi.org/10.1111/1541-4337.12006

458 Wannatong, L., Sirivat, A., & Supaphol, P. (2004). Effects of solvents on electrospun polymeric
459 fibers: preliminary study on polystyrene. Polymer International, 53(11), 1851–1859.
460 https://doi.org/10.1002/pi.1599

461 Yalkowsky, S. H., He, Y., & Jain, P. (2010). Handbook of aqueous solubility data. Second ed. CRC
462 Press Taylor and Francis Group.

463   Yu, D.-G., Li, X.-X., Ge, J.-W., Ye, P.-P., & Wang, X. (2013). The Influence of Sheath Solvent's Flow

464   Rate on the Quality of Electrospun Ethyl Cellulose Nanofibers. Modeling and Numerical

465   Simulation of Material Science, 03(04), 1–5. https://doi.org/10.4236/mnsms.2013.34B001

466

467 **Table 1.** Process parameters and microscopic observations of the material obtained during ES of

468 solutions with 15 % PLA in different binary solvent systems. Boiling point of each solvent

469 (Smallwood, 1996) was indicated in brackets.

Solvents ratio (v/v)				Flowrate (µL/h)		Distance to collector (cm)	Micro-structure in Figure 1	Process time* (min)
EtAc (77 °C)	GAA (118 °C)	ButAc (126 °C)	DMSO (189 °C)	through interior needle	through exterior needle			
0	0	0	1	1000	0	20	A	>60
0	0	0	1	1000	15	20	B	>60
1	0	0	1	1000	0	20	C	>60
1	0	0	1	1000	25	20	D	>60
1	0	0	3	1000	0	20	E	>60
2	0	0	3	1000	0	20	F	>60
1	0	1	0	1100	0	15	G	~ 10
1	1	0	0	1200	0	15	H	~ 13
1	1	0	0	1100	100	15	I	~ 20

470 *without solidification at the injector tip

471

472   **Table 2.** Encapsulating efficacy (EE) values expressed as % of encapsulated CA referred to the

473   initial amount and final carvacrol content (g / g polymer) in the electrospun and cast materials

474   using different solvent systems. The different letters (superscripts) in each column indicate

475   significant differences (p<0.05) between the samples.

476

Solvent system	EE (%)		Carvacrol content (g /g PLA)	
	ES	Casting	ES	Casting
EtAc:DMSO (0:1)	52 ± 4^a	78 ± 4^a	0.103 ± 0.008^a	0.156 ± 0.008^a
EtAc:DMSO (1:3)	62 ± 6^b	89 ± 6^b	0.124 ± 0.013^b	0.177 ± 0.012^b
EtAc:DMSO (2:3)	68 ± 2^b	76 ± 3^a	0.136 ± 0.005^b	0.151 ± 0.005^a

477

478   **Table 3**. Thermal degradation temperatures (T_o – onset temperature at which degradation

479   begins, T_p – peak temperature at maximum degradation rate), and mass fraction released in the

480   first stage (M) before the polymer degradation step. The superscript letters indicate significant

481   differences ($p<0.05$) between the formulations with or without carvacrol in the respective

482   columns.

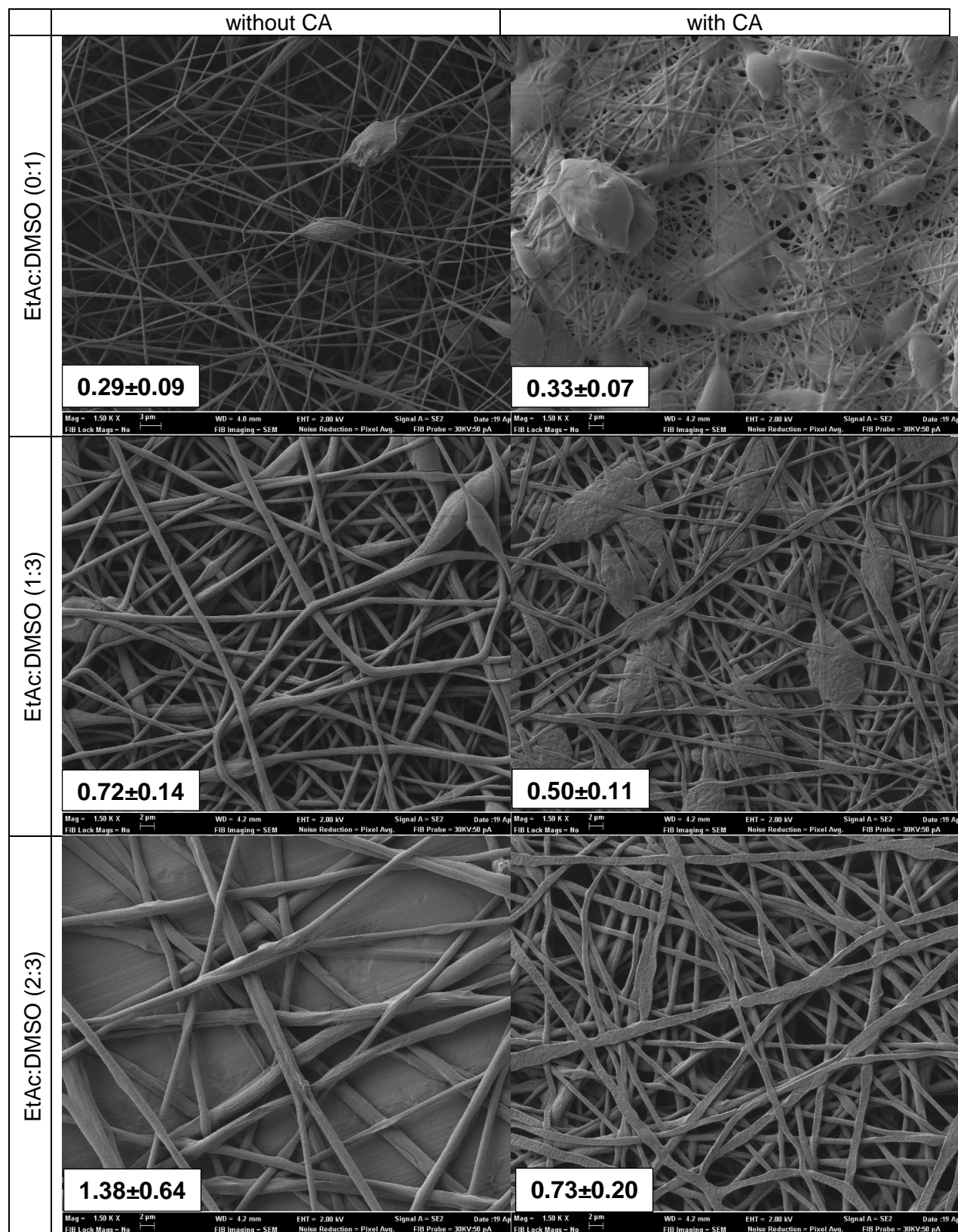| Sample			First peak		Second peak		M
			T_o (°C)	T_p (°C)	T_o (°C)	T_p (°C)	(g/g sample)
Casting	with CA	EtAc:DMSO (0:1)	34±2[a]	131±16[ef]	234±5[a]	283±4[ab]	0.13
		EtAc:DMSO (1:3)	34±3[a]	141±12[f]	235±29[a]	287±25[ab]	0.17
		EtAc:DMSO (2:3)	35±4[a]	141±6[f]	272±1[cd]	320±1[d]	0.17
	without CA	EtAc:DMSO (0:1)	35±3[a]	73±5[a]	291 ±1[de]	327±1[d]	0.02
		EtAc:DMSO (1:3)	35±4[a]	96±7[abc]	264±7[bc]	304±9[c]	0.16
		EtAc:DMSO (2:3)	35±2[a]	76±23[a]	250±25[ab]	297±17[bc]	0.01
ES	with CA	EtAc:DMSO (0:1)	39 ±1[ab]	178±2[g]	242±3[a]	291±3[abc]	0.04
		EtAc:DMSO (1:3)	36±2[ab]	131±17[ef]	233±2[a]	280±1[a]	0.05
		EtAc:DMSO (2:3)	35±3[a]	125±22[def]	238±8[a]	289±6[abc]	0.03
	without CA	EtAc:DMSO (0:1)	43±5[bc]	106±25[bcd]	281±8[cde]	323±4[d]	0.14
		EtAc:DMSO (1:3)	48±9[c]	88±15[ab]	292±5[e]	328±2[d]	0.23
		EtAc:DMSO (2:3)	76±7[d]	116±4[cde]	290±5[de]	326±2[d]	0.46
Carvacrol			118±15	159±7	-	-	-
PLA pellet			-	-	272±4	311±4	-

483

484   **Table 4.** Glass transition temperature (T_g) obtained from different heating and cooling steps of

485   the DSC thermograms for the different samples. The superscript letters indicate significant

486   differences ($p < 0.05$) between the formulations in the same column.

| Sample			T_g (°C)		
			First heating	**Cooling**	**Second heating**
Casting	PLA + CA	EtAc:DMSO (0:1)	15 ± 1^b	23 ± 1^a	26 ± 1^a
		EtAc:DMSO (1:3)	19 ± 2^c	35 ± 2^b	37 ± 2^b
		EtAc:DMSO (2:3)	8 ± 4^a	17 ± 4^a	20 ± 5^a
	PLA	EtAc:DMSO (0:1)	45 ± 2^i	41 ± 1^{bcd}	44 ± 1^{cd}
		EtAc:DMSO (1:3)	40 ± 1^{fg}	46 ± 1^{cde}	49 ± 1^{de}
		EtAc:DMSO (2:3)	44 ± 3^{gh}	52 ± 1^e	55 ± 1^e
ES	PLA + CA	EtAc:DMSO (0:1)	35 ± 1^e	37 ± 3^{bc}	39 ± 4^{bc}
		EtAc:DMSO (1:3)	30 ± 1^d	34 ± 1^b	36 ± 2^c
		EtAc:DMSO (2:3)	30 ± 2^d	39 ± 7^{bc}	41 ± 7^{bcd}
	PLA	EtAc:DMSO (0:1)	39 ± 2^{ef}	46 ± 8^{de}	49 ± 7^{de}
		EtAc:DMSO (1:3)	40 ± 5^f	39 ± 3^{bcd}	41 ± 3^{bcd}
		EtAc:DMSO (2:3)	37 ± 1^{ef}	–	–
PLA pellet			56	52	55

487
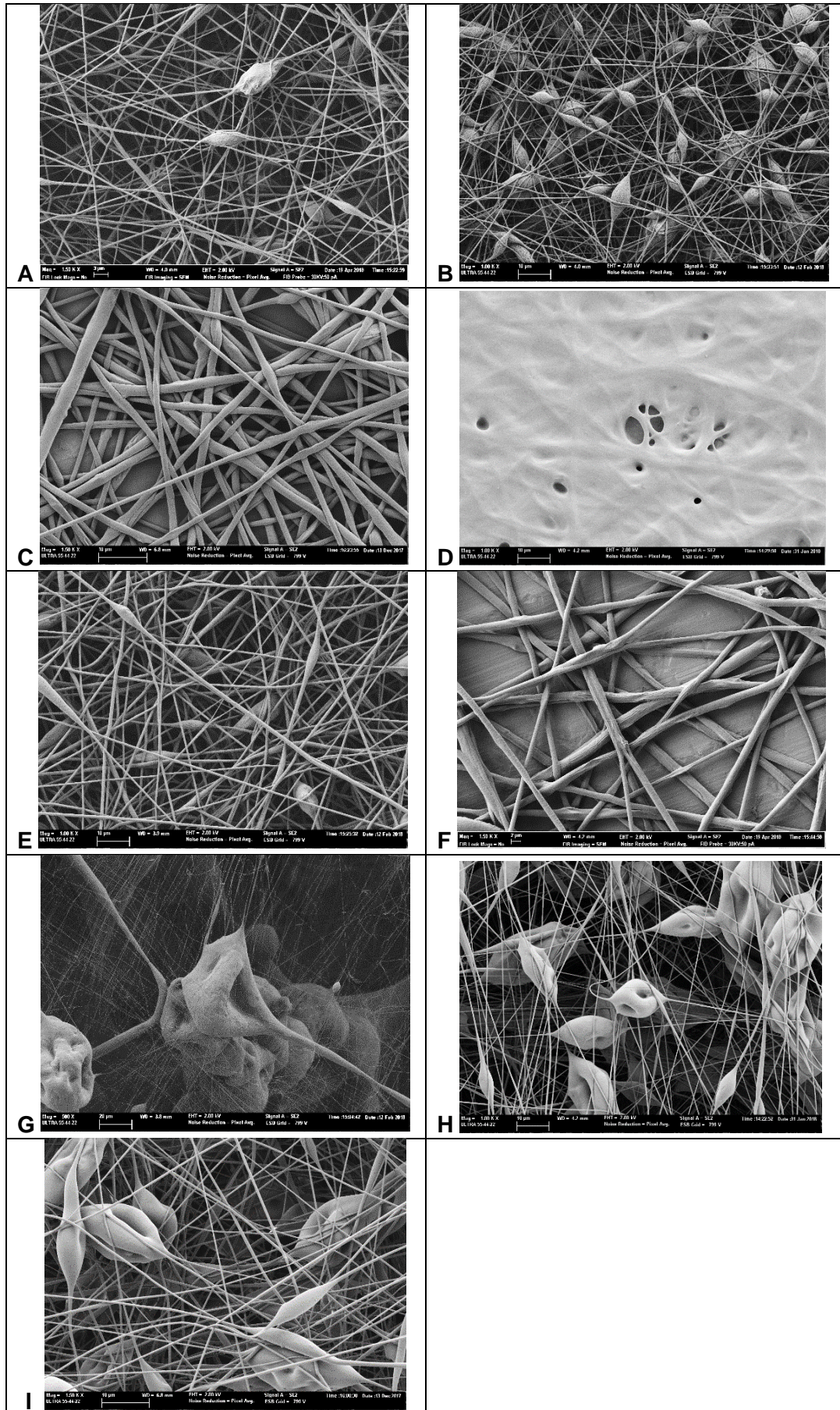
488 **Figure 1**. Microstructure of the electrospun PLA material using the different solvent systems and

489 process conditions described in **Table 1**.

	without CA	with CA
EtAc:DMSO (0:1)	0.29±0.09	0.33±0.07
EtAc:DMSO (1:3)	0.72±0.14	0.50±0.11
EtAc:DMSO (2:3)	1.38±0.64	0.73±0.20

Figure 2. FESEM micrographs of the electrodeposited material, with and without carvacrol. Magnification of 1500x. Estimated mean values of fiber diameters (µm) were specified for each sample.
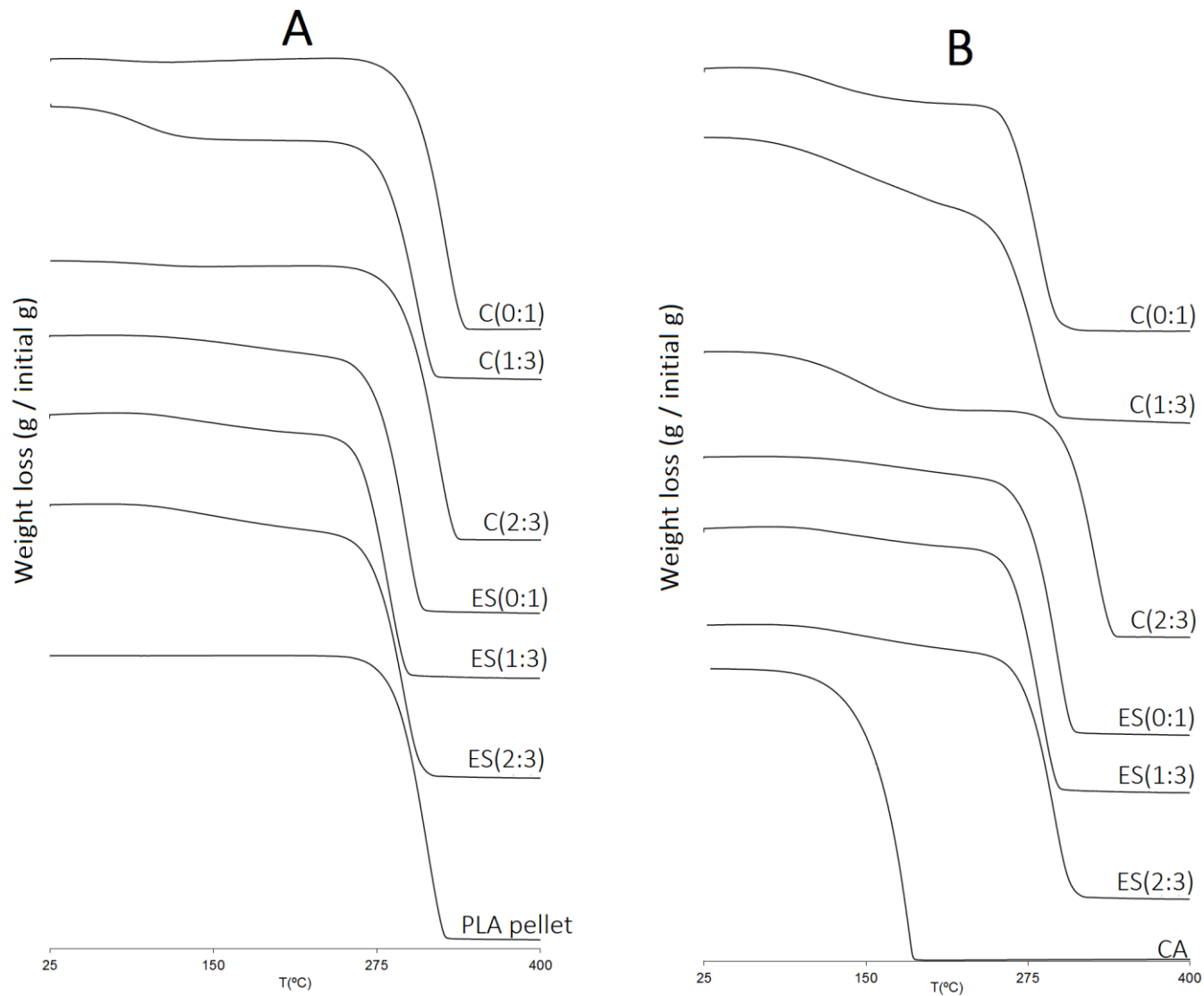
Figure 3. TGA curves of the cast (C) and electrospun (ES) PLA materials, using different EtAc:DMSO ratios (0:1, 1:3 and 2:3). A: samples without carvacrol, B: samples encapsulating carvacrol.

495
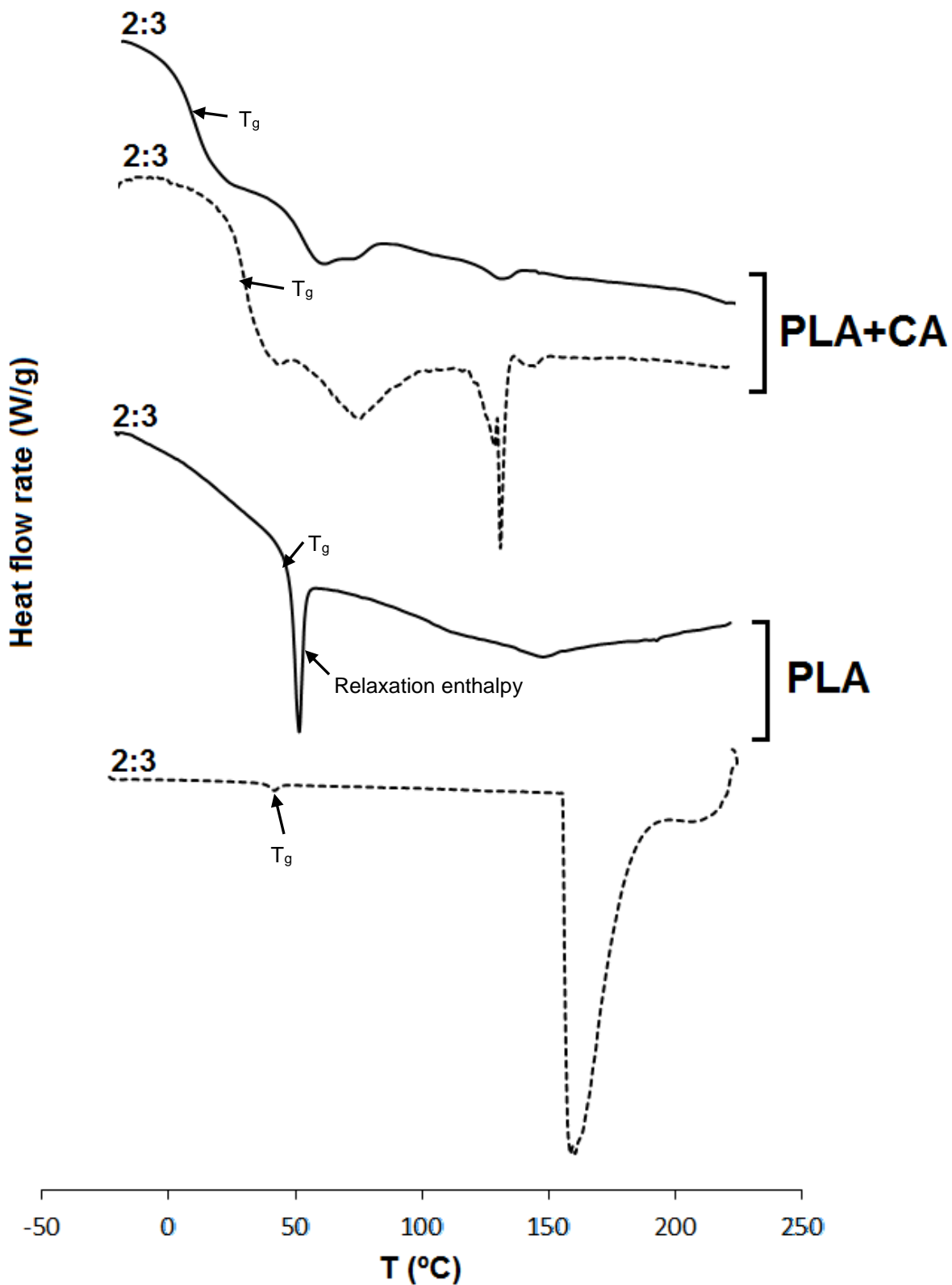
Figure 4. DSC thermograms (first heating scan) of PLA materials obtained from the EtAc:DMSO (2:3) solution by casting (continuous line) or electrospinning (dashed line). Endothermic events are attributable to the evaporation of the retained solvent in the sample.